Structural Engineering and Mechanics, *Vol. 71, No. 4 (2019) 407-416*
DOI: https://doi.org/10.12989/sem.2019.71.4.407

Behaviours of steel-fibre-reinforced ULCC slabs subject to concentrated loading

Jun-Yan Wang[1a], Xiao-Long Gao[1b] and Jia-Bao Yan[*2],

[1]*Key Laboratory of Advanced Civil Engineering Materials, Tongji University, Ministry of Education, Shanghai 201804, P.R. China*
[2]*School of Civil Engineering, Tianjin University, Tianjin 300350, P.R. China*

(Received September 15, 2018, Revised April 9, 2019, Accepted April 10, 2019)

Abstract. Novel steel fibre reinforced ultra-lightweight cement composite (ULCC) with compressive strength of 87.3MPa and density of 1649kg/m^3 was developed for the flat slabs in civil buildings. This paper investigated structural behaviours of ULCC flat slabs according to a 4-specimen test program under concentrated loading and some reported test results. The investigated governing parameters on the structural behaviours of the ULCC slabs include volume fraction of the steel fibre and the patch loading area. The test results revealed that ULCC flat slabs with and without flexure reinforcement failed in different failure mode, and an increase in volume fraction of the steel fibre and loading area led to an increase in flexural resistance for the ULCC slabs without flexural reinforcement. Based on the experiment results, the analytical models were developed and also validated. The validations showed that the analytical models developed in this paper could predict the ultimate strength of the ULCC flat slabs with and without flexure reinforcement reasonably well.

Keywords: ULCC; flexural resistance; fibre reinforced concrete; flat slab; analytical model

1. Introduction

ULCC is cement-based composite material with light weight and high-strength, and this type of material has been developed for civil and offshore constructions in recent years (Wang *et al.* 2013, Chia *et al.* 2011, Wang *et al.* 2014, Liu *et al.* 2012). The characteristic of light weight for ULCC is achieved according to the using of cenosphere as the micro-lightweight aggregates (Wang *et al.* 2013, Chia *et al.* 2011). The cenosphere is a type of hollow sphere, with a diameter between 10μm and 300 μm, the thickness of cenosphere is about 2.5~10.5% of its diameter. In addition, the cenospheres used in the ULCC are the combustion by products of the coal-fired thermal power plants. Thus, reusing the cenospheres could save energy and reduce the carbon dioxide emissions (Wang *et al.* 2013, Chia *et al.* 2011, Wang *et al.* 2014). The ULCC was originally developed for the steel-concrete composite structure (Sohel *et al.* 2011, Sohel *et al.* 2013) and steel-concrete-steel (SCS) sandwich composite structures (Yan *et al.* 2014, Yan *et al.* 2015,). With the advantages high specific strength which is about 47 kPa/kg m-3, the ULCC can be also used to develop the flat slabs in the office and residential building, high-rise building, and parking buildings that would greatly reduce the self-weight of the structure and improve the seismic performance of buildings.

The slab-column system consists of flat slabs and supported columns, which has a great competition for civil buildings in terms of easy construction, architectonical flexibility and easy installation and placement (Delahay and Christopher 2007). Despite these advantages of the flat slab system, all over the world, several dramatic collapses have taken place as punching shear failure over the past decades (Gardner *et al.* 2002). The failure of punching shear occurred in the joint of flat slab and the supported column probably triggered the sudden collapse of the building (Schousboe 1976), e.g., in May 16, 1968, at Ronan Point apartment, the punching shear failure of the slabs caused by the explosion triggered the successive damage of the floors. Therefore, this type of failure mode needs to be paid attention to, and the punching shear resistance of the flat slabs needs to be experimentally and analytically studied. Many researchers have study the punching shear resistance of concrete flat slabs (Rankin and Long 2015, Alexander and Simmonds 1987, Yankelesky and Leibowitz 1999 Kankam and Odum 2006, Heodorakopoulos and Swamy 2002). However, most of these researches concentrate on the flat slab with normal weight concrete.

Compared with the normal weight concrete, the novel steel fibre reinforced ULCC with density around 1650kg/m^3 and compressive strength around 85MPa developed for the flat slabs could save 33% of the self-weight under the same strength. This new ULCC achieves better balance between strength and density than the first generation of ULCC which has the compressive strength of 60 MPa and density of 1400kg/m^3. The elastic modulus of this new ULCC reaches 20 GPa, which is amount to the normal weight concrete of low strength grades. For the applications of the ULCC, previous researches mainly focused on the structure behaviours of the steel-concrete (SC) or steel-concrete-steel (SCS) composite structures. And For the ULCC used in flat

*Corresponding author, Ph.D.
E-mail: ceeyanj@163.com
[a] Ph.D.
[b] Ph.D.

http://www.techno-press.com/journals/sem&subpage=7
ISSN: 1225-4568 (Print), 1598-6217 (Online)

slab structure, Yan *et al*. (2016) studied the punching shear resistance of ULCC flat slab with reinforcement according to the experiments of 14 ULCC flat square slabs under concentrate load. However, few researches about the resistance of ULCC flat slab without reinforcement have been reported. Therefore, it is of interest to develop the flat slabs with high performance ULCC materials that further improves their structural performances and increases the construction efficiency. Thus, with the developments of the flat slabs with high performance ULCC, it is necessary to obtain more information on the flexural resistance on this type of structure using this new class of ULCC. Analytical model including punching shear resistance and flexural resistance also should be developed based on more test data.

This paper aimed to study the structure behaviours of the steel fibre reinforced ULCC flat slabs without flexure reinforcement under concentrated loading and the development of design approaches on the ultimate strengths of ULCC flat slabs with and without flexure reinforcement. The class of ULCCs with compressive strength around 85 MPa and density around 1650 kg/m^3 were used in the flat slabs. This paper reported a test program that consisted of four two-way flat slabs made of ULCC with steel fibres. All these slabs were tested under patch loading that simulated the concentrated force transferred from the supporting column. The experimental results reported detailed information on the load-transfer mechanism, load-deflection performances and failure modes. Including the experimental studies, this paper also developed analytical model on flexure resistance of ULCC flat slabs with and without flexure reinforcement. A design approach on both punching shear resistance and flexure resistance of this structure was also developed. And the accuracies of the design equations were confirmed through comparisons with the test results. Based on these validations, the prediction methods were finally recommended on the ultimate strength for the steel-fibre reinforced ULCC flat slabs.

2. Test program

2.1 ULCC, steel fibres and reinforcements

ULCC consists of water, ordinary Portland cement, cenospheres, chemical admixtures, silica fume, and straight steel fibres. The density of cenosphere used for the ULCC in this paper is 870 kg/m^3. The workability was ensured according to the superplasticizer (ADVA® 181) as the low water-to-binder ratio. The shrinkage strains and air contents were reduced according to the using of shrinkage-reducing admixture (Eclipse® Floor). The tensile toughness of the ULCC is improved according to the using of steel fibre. The properties of the steel fibre used in this paper are listed in Table 1. The length of straight steel fibre is 6 mm and the diameter of straight steel fibre is 0.16 mm. ULCC with the volume fractions of steel fibre, i.e., 0.5%, 1.0%, and 2.0% was developed in this paper, which was used to investigate the effect of the content of steel fibre on the ultimate strength behaviour of the ULCC flat slab.

Mix proportion of the ULCC with density of 1600 kg/m^3 was designed accordingly to the method developed by Wang *et al*. (2014). The mix proportions of the ULCC used in this paper are listed in Table 2. The compressive and tensile stress-strain relations of the ULCC with different steel fibre contents are depicted in Fig. 1(a) and Fig. 1 (b) respectively. The compressive stress-strain curves were recorded from the compression tests, and the compression test specimens are cylinders with the diameter of 100mm and the height of 200mm which is based on the code of ASTM C39/C39M (2014). The tensile stress-strain curves were recorded from the direct tensile tests. Fig. 2(b) shows the set-up for the direct tensile test. Table 3 lists the detailed mechanical properties of ULCC used for the design of ULCC slab specimens involved in this paper.

Table 1 Detail properties of the steel fibre

d (mm)	L (mm)	Aspect ratio	Density (g/cm^3)	Tensile strength (MPa)	Elastic modulus (GPa)
0.16	6	37.5	7.8	2500	200

The diameter of ribbed longitudinal reinforcing steel bar used in the ULCC flat slab is 12mm. The longitudinal reinforcing steel bars were tested accordingly to ASTM A370-13 (2013) to obtain the mechanical properties. The average yield strength of the longitudinal reinforcing steel bar is 496.5 MPa. The average elastic modulus is 201.8 GPa.

2.2 Flat slab specimens

Four slab specimens namely S1~S4 in total were prepared in this test program, among which one specimen S4 adopted the reinforcements mesh and the rest three specimens S1~S3 did not adopt any reinforcement. For the four specimens S1~S4, the investigated parameters include the volume fraction of the steel fibres and the width of the loading area. Test specimens S1, S2, and S3 adopted different volume fraction of the steel fibres of 0.5%, 1% and 2%, which were used to assess the influence of the of steel fibre contents. Test specimen S5~S8 adopted reinforcement mesh, which were cited from the test results reported by Yan *et al*. (2016). And the test specimen S5 was used to compare with S1 to investigate the influence of flexural reinforcements. Test specimen S4 was loaded under the square loading area with width of 125 and test specimen S5 was loaded under the square loading area with width of 100 mm, which was used to investigate the influence of loading area.

The fresh ULCC was poured into the wooden mould after the arrangement of the longitudinal reinforcing steel bar mesh. The thickness of concrete cover the flat slab specimen is 10mm. All the specimens adopted no shear reinforcements. For each specimen, six cylinders were casted at the same day of casting the specimen to obtain the density, compressive and tensile strength of specimen, three specimens for the direct tensile test showed in Fig. 2(a) and Fig. 2 (b) were casted to obtain the direct tensile strength. All the specimens and the corresponding cylinders were tested on 28 days after the casting. Fig. 3 illustrates the geometry of the flat slabs. The width of loading area, the

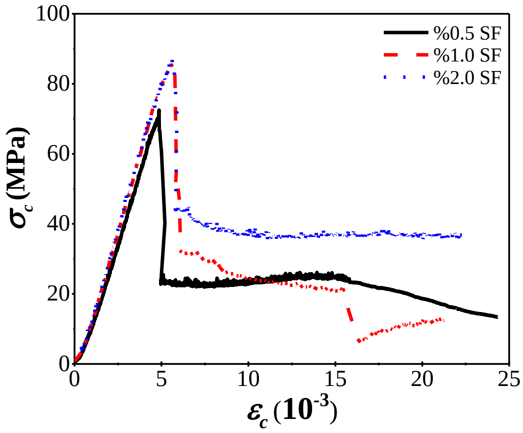

(a) Compressive stress-strain relations

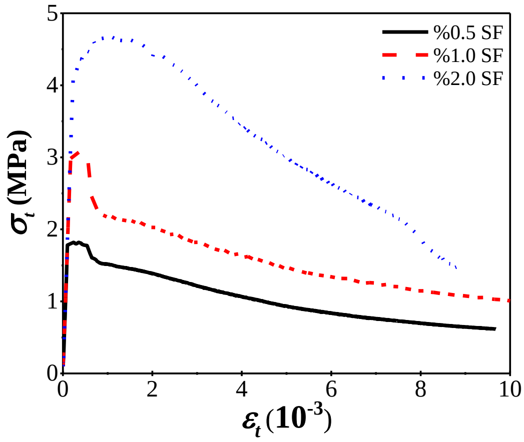

(b) Tensile stress-strain relations

Fig. 1 Stress-strain curves of ULCC with different steel fibre content

Table 2 Mix proportions of ULCC (kg/m^3)

Test specimen	OPC	Water	Cenosphere (QK300)	Silica fume	SRA	Steel Fibre (SF)	SP ADVA181
S1	873.9	264.94	287.59	97.1	9.29	39	7.5
S2	873.9	264.94	287.59	97.1	9.29	78	7.5
S3,S8	873.9	264.94	287.59	97.1	9.29	156	7.5
S4	873.9	264.94	287.59	97.1	9.29	78	7.5
S5~S6	873.9	264.94	287.59	97.1	9.29	78	7.5
S7	873.9	264.94	287.59	97.1	9.29	0	7.5

OPC denotes ordinary Portland cement; SRA denotes shrinkage reduction; SP denotes the superplasticizer;

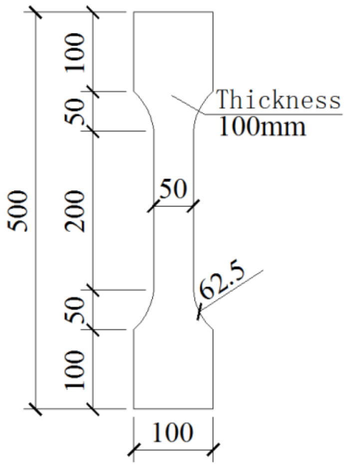

(a) Configuration of coupon

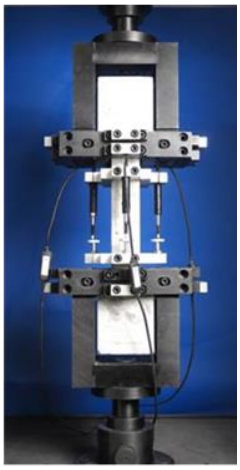

(b) Test set-up

Fig. 2 Test set-up for ULCC direct tension test

thickness of flat slab and material properties of the four specimens are listed in Table 3.

2.3 Test set-up and instrumentations

Fig. 3 shows the test set-up for the ULCC flat slab test specimen and the slabs were supports along the four edges. The clear span for each slab is 600 mm. The concentrate load was conducted according to an INSTRON hydraulic jack located at geometry centre of the specimens according to. Displacement control method with the loading rate of 0.1 mm/min was applied in this paper. Five linear variable displacement transducers (LVDTs) showed in Fig. 3 were installed to monitor the deflections at the centre and 130 mm off the centre. The initiation and development of cracks in the top and bottom surface of the slab was observed during the course of the test. The tests terminated until the platen punched through the slab. All the reaction forces and deflections were automatically recorded at different loading levels.

Table 3 Details of the flat slabs with ULCC

Slab	Data Resourse	a (mm)	h (mm)	ρ_{fl} (mm)	ρ_{SF} (%)	f_{ck} (MPa)	E_c (MPa)	f_{tk} (MPa)	f_{tp} (MPa)	ε_{tk} (10^{-3})	Density (kg/m^3)
S1	This paper	100	90	0.0	0.5	72.5	19.0	1.85	3.2	0.16	1590
S2		100	90	0.0	1.0	86.1	19.8	3.07	4.5	0.18	1595
S3		100	90	0.0	2.0	87.3	20.3	4.13	6.2	0.24	1690
S4		125	90	1.71	1.0	65.8	19.8	3.07	4.4	0.18	1595
S5	Yan *et al.* (2016)	100	90	1.71	1.0	87.3	19.9	-	4.6	-	1648
S6		100	70	1.70	1.0	85.3	19.7	-	4.5	-	1590
S7		100	90	1.71	0.0	78.6	18.9	-	1.2	-	1561
S8		100	90	1.71	2.0	82.4	20.3	-	6.2	-	1690

*a denotes width of the loading area; h denotes depth of flat slab section; ρ_{fl} denotes the longitudinal reinforcing steel bar ratio; ρ_{SF} denotes volume fraction of the steel fibres; f_{ck} denotes the compressive strength; f_{tk} denotes the direct tensile strength; f_{tp} denotes the splitting tensile strength. ε_{tk} denotes the tensile strain before the sudden drop of tensile stress-strain curve.

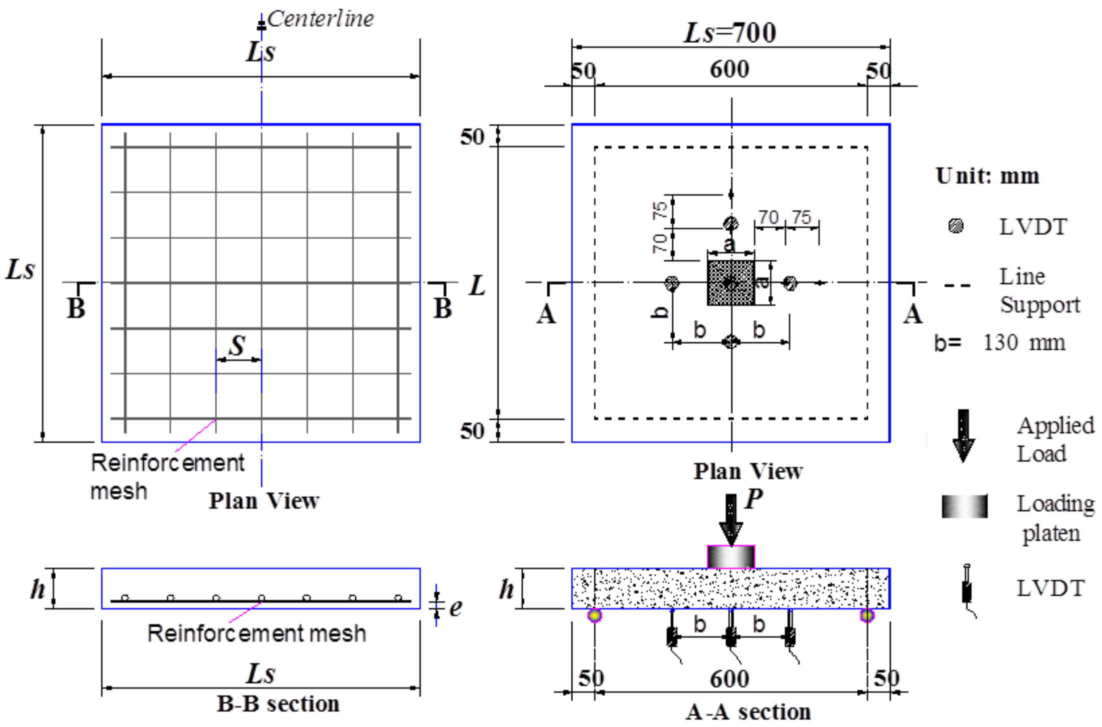

(a) Geometric details and layout of instrumentations

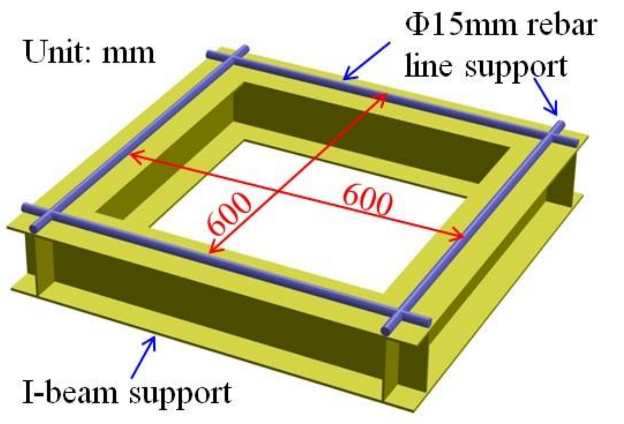

(b) Support

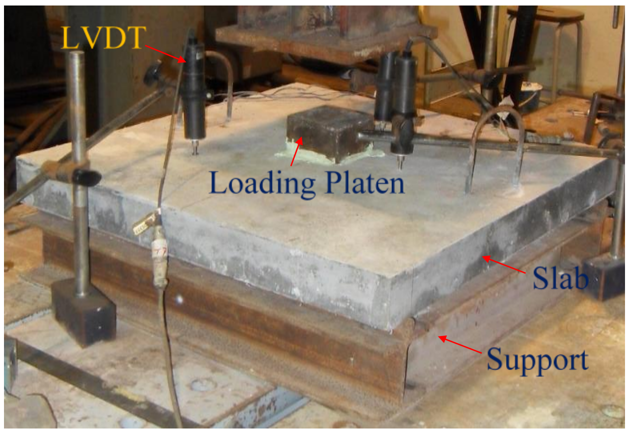

(c) Test setup

Fig. 3 Dimension and test set-up for flat slab specimen

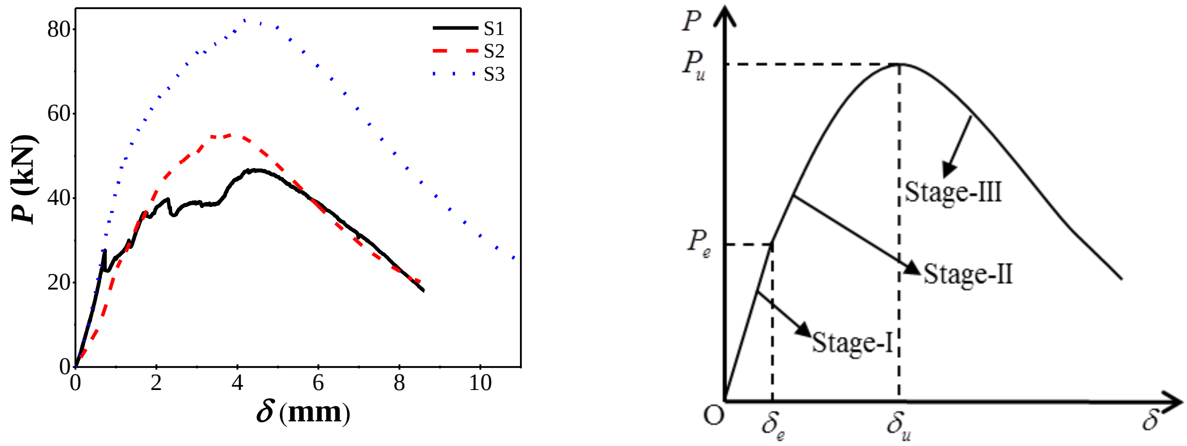

(a) Load-central deflection curves (b) Typical load-central deflection curves

Fig. 4 Load-central deflection relations for ULCC slabs under concentrated loads

(a) S2 top surface (b) S2 bottom surface

Fig. 5 Typical crack patterns of the specimen without reinforcement

3. Test results and discussions

3.1 Failure mode of ULCC slabs without reinforcement

Load-deflection curves of the test slabs S1~3 without flexural reinforcement were shown in Fig. 4. As seen from Fig. 4, the load-deflection curves of ULCC slabs without reinforcement generally includes three distinct stages, which is different from the four stages for the ULCC slabs with reinforcement (Yan *et al*. 2016). At stage I, the slab behaved elastically, i.e., the applied load increased linearly as the central deflection. As the deflection increases, at stage II, there were some cracks appeared in the bottom surface of the ULCC slab. Since the ULCC matrix starts to crack, the tensile stresses are transferred to the steel fibres between the cracks and those fibres bridge the cracks. These bridging fibres enhance the bearing capacity the slabs, which permitted the slab taking more loads after the appearance of cracks. At the second stage, this tensile stresses between cracks were transferred by the steel fibres until the steel fibres were pulled out from the matrix. The tensile capacity depends on the adhesion strength between the cement matrix and the fibres. When the load is complete, there was no tensile fracture failure of steel fibres observed from the tests. As the cracking of flat slab and bond failure of steel fibres, the slabs behaved nonlinearly at stage II. And more cracks appeared in the bottom surface and extended from the centre to the corner of the slabs as the increasing of loading. Finally, the slabs achieve their ultimate resistances Fig. 5(a)~(b) depicts the representative specimen after the loading in this paper. The distribution of cracks for the slab S2 which was the representative slab without reinforcement were showed in Fig. 5(a)~(b). Fig. 6(a)~(b) depicts the distribution of cracks for S5 (Yan *et al*, 2016) which was the representative slab with reinforcement. As showed in Fig. 5 and Fig. 6, three are no punching cone observed in the top surface for the ULCC slabs without reinforcement, which is different from the failure mode of ULCC slabs with reinforcement. These failure phenomena implied that the ULCC slabs without reinforcement failed in flexure mode and the ULCC slabs with reinforcement failed in punching shear mode.

The ultimate resistances of the five flat slabs are listed in Table 4. And these values were determined by the minor value of punching shear resistance and flexural bending resistance. For the flat slabs with flexural reinforcement, their flexural bending resistance were enhanced by these reinforcements and larger than the punching shear resistance of the slab, which resulted in punching shear failure mode. And vice versa, for the slabs without flexural reinforcement, as the punching shear resistance is greater

(a) S5 top surface (b) S5 bottom surface

Fig. 6 Crack patterns of the specimen with reinforcement

Table 4 Ultimate resistances obtained from test results and analytical model

Test	Data Resourse	δ_u (mm)	P_u (kN)	Failure mode	K_e (kN/mm)	$P_{u,R}$ by Eq.8 (kN)	$\frac{P_u}{P_{u,R}}$	$P_{u,f}$ by Eq. 2 (kN)	$\frac{P_u}{P_{u,f}}$	$P_{u,T}$ by Eq.12 (kN)	$\frac{P_u}{P_{u,T}}$
S1		4.4	46.7	FL	34.9	126.7	0.37	38.6	1.21	38.6	1.21
S2	This paper	3.4	55.3	FL	35.5	179.2	0.31	58.8	0.94	58.8	0.94
S3		4.3	82.3	FL	40.8	263.3	0.31	79.5	1.04	79.5	1.04
						Mean	0.33		1.06		
S4	This paper	4.1	151.1	PS	51.0	143.9	1.05	328.2	0.46	143.9	1.05
S5		4.1	146.5	PS	38.9	150.3	0.97	330.2	0.44	150.3	0.97
S6	Yan *et al*. (2016)	3.8	102.1	PS	28.3	91.1	1.12	329.0	0.22	91.1	1.12
S7		2.6	72.0	PS	26.5	77.7	0.93	329.5	0.51	77.7	0.93
S8		4.1	167.5	PS	42.1	212.4	0.79	328.2	0.46	212.4	0.79
						Mean	0.97		0.42		
In total										Mean	1.01

* FL denotes flexural failure mode; PS denotes punching shear failure mode;

than flexural bending resistance, thus the ULCC flat slabs failed in flexural mode.

3.2 Discussions of experimental results

The values of ultimate resistance, P_u, the corresponding deflection, δ_u, and the stiffness, K_e, for each test are listed in Table 4. The stiffness of the ULCC slab is defined as follows:

$$K_e = \frac{P_e}{\delta_e} \tag{1}$$

where P_e denotes the resistance at the elastic stage of the load-central deflection curves and δ_e denotes corresponding central deflection. In this manuscript, P_e adopts 50% of the ultimate resistance in the elastic stage of the load-central deflection curves.

3.2.1 Effect of steel fibre content in ULCC

Fig. 7 (a) and Fig. 7(b) depict the influences of volume fraction of steel fibre, ρ_{SF}, on P_u and K_e for specimens without flexural reinforcement, respectively. The ultimate resistance of the slab, P_u, increases from 46.7 kN to 55.3 kN and 82.3 kN as ρ_{SF} increases from 0.5% to 1% and 2%, respectively; meanwhile, the stiffness, K_e, increases from 34.9 kN/mm to 35.5 kN/mm and 40.8 kN/mm, respectively.

Fig. 7(c) shows the effects of ρ_{SF} on the compressive strength of ULCC. ρ_{SF} has ignorable influence on compressive strength of the ULCC. Fig. 7(d) shows the effects of ρ_{SF} on the direct tensile strength of the ULCC. Unlike the influences on compressive strength, ρ_{SF} has significant positive influence on the tensile strength of the ULCC. For the slab without flexural reinforcement, adopting higher steel fibre content improves the tensile strength of the ULCC, which increases the flexural bending resistance of the cross section and increases flexural bending resistance of the ULCC slab. Therefore, the influence of the steel fibre content should be included in the analysis of the ultimate loading carrying capacity of the ULCC slab.

3.2.2 Effect of loading area

Slabs S4 and S5 are designed with the same materials and geometry. However, the slabs have different square loading areas, the side width of loading area for slabs S4 is 100mm, and the side width of loading area for slabs S5

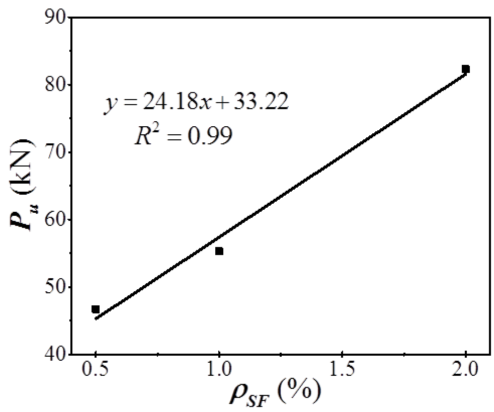

(a) Effect of ρ_{SF} on P_u

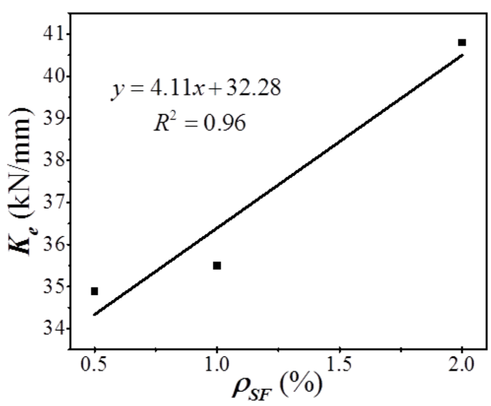

(b) Effect of ρ_{SF} on K_e

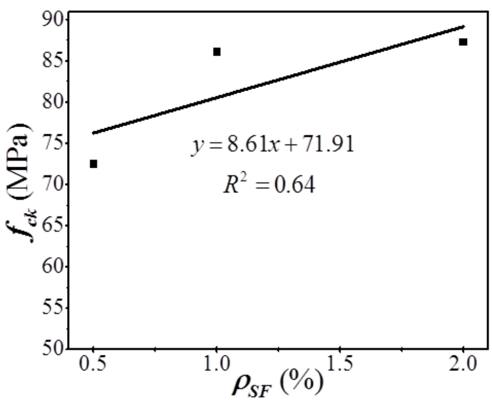

(c) Effect of ρ_{SF} on compressive strength

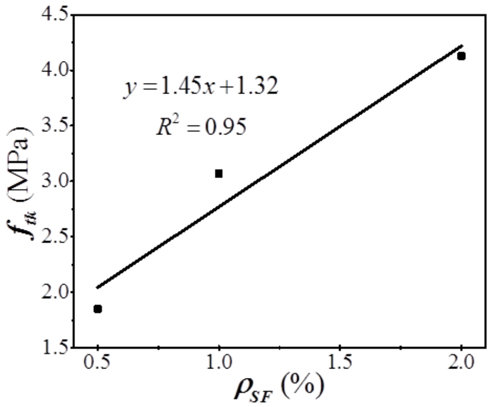

(d) Effect of ρ_{SF} on tensile strength

Fig. 7 Effects of different parameters

is 125mm. Fig. 8 and Table 4 show that P_u slightly increases by 3% from 146.5 kN to 151.1 kN and K_e significantly increases by 31 % from 38.9 kN/mm to 51.0 kN/mm as a increased from 100 mm to 125 mm. Considering the variations of the strength of the ULCC used in S4 and S5, the ratio, $P_u/(h_e\sqrt{f_{ck}})$, is used to eliminate the influence of the section strength and the depth of the ULCC. $P_u/(h_e\sqrt{f_{ck}})$ is proportional to the critical perimeter. The $P_u/(h_e\sqrt{f_{ck}})$ ratios for slabs S4 and S5 are 232 and 196, respectively, which increases about 18% as a increased from 100 mm to 125 mm. Therefore, increasing the control perimeter for the punching cone helps improve the punching shear resistance of the ULCC slab. Moreover, the increasing of loading area reduces the effective span that leads to larger stiffness in the load-deflection curves.

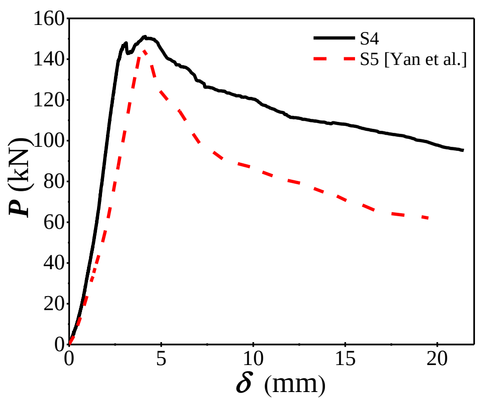

Fig. 8 Load-central deflection curves for test slabs S4 and S5

4. Analysis on ultimate strength of ULCC slab with and without flexural reinforcement

Yan *et al*. (2016) investigated the strength behaviours of ULCC flat slabs with flexural reinforcement under concentrate load according to experiment method. And the structural behaviours of ULCC flat slabs without flexural reinforcement has been analysed. However, the flexural failure of ULCC flat slab without flexural reinforcement is different from the punching failure mode for ULCC flat slab with flexural reinforcement. And more comprehensive design approaches still need to be built to ensure the safety of ULCC flat slab.

4.1 Flexure resistance of slabs

For the flexural resistance, the yield line method maybe used to predict their ultimate resistances. Ward (2010) proposed a formula to predict this flexural resistance of the slabs with the fibres as the following

$$P_{u,f} = 7.45m_{cr} \tag{2}$$

where m_{cr} is the bending moment resistance in unit width.

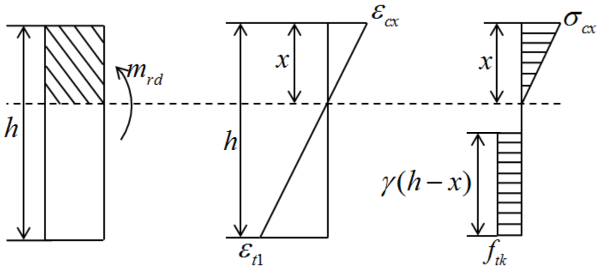

Fig. 9 Bending resistance of a ULCC flexural member without reinforcement (Wang *et al*. 2018)

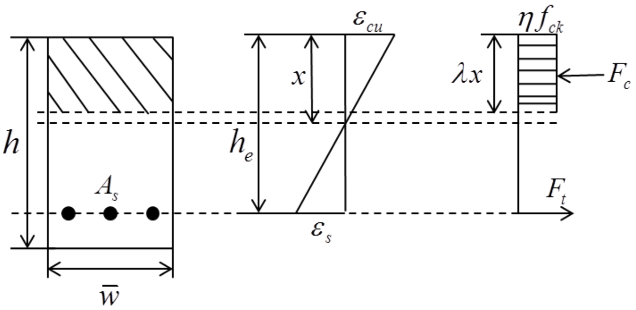

Fig. 10 Determination of the flexural bending resistance of the cross section for the slab with reinforcement

1) For the slabs without flexural reinforcement

The analytical model for ultimate resistance of ULCC members in simple bending has been developed by Wang *et al*. (2018). Fig. 9 shows the carrying capacity model of bending moment of ULCC flexural member, and bending moment resistance of ULCC, m_{rd}, can be determined as (Wang *et al*. 2018).

$$m_{rd} = (\gamma - 0.5\gamma^2)\sigma_{t1} b(h-x)^2 + \frac{E\varepsilon_{t1}x^3}{3(h-x)}b \tag{3}$$

where, σ_{tl} denotes the tensile strength; ε_{tl} denotes the tensile strain at the end of plateau stage in the tensile stress-strain curves; b denotes the width of ULCC flexural member. γ denotes the parameter which influences the height of tension zone of ULCC flexural member. The parameter γ could be validated according to the experiment results. According to the parametric study, the test results and the analytical results are in good agreement when γ equal to 0.9.

2) For the slabs with flexural reinforcement

Fig. 10 plots the stress and force distribution of the cross section of the flat slabs. According to the stress distribution in Fig. 10, m_{cr} can be determined as the following:

$$m_{cr} = f_y \rho_{fl} h\bar{w}\left(h_e - 0.5\lambda x\right) \tag{4}$$

The force equilibrium equation for the cross section showed in Fig. 10 can be defined as the following:

$$\lambda x \cdot \eta f_{ck} = \min\left(E_s\varepsilon_{cu}\frac{h_e - x}{x}, f_y\right)A_s \tag{5}$$

where, ρ_{fl} denotes flexural reinforcing ratio; f_y denotes yield strength of the reinforcement; h denotes the nominal depth of the cross section of the slab; h_e denotes and effective depth of the cross section of the slab; $\bar{w}$ denotes unit width of the slab; x denotes depth of the neutral axis of the cross section, which can be determined through solving Eq. (5); λ denotes the factor used to define the effective height of compression zone which can be determined by Eq. (6); η denotes the factor used to correct the compressive strength which can be determined by Eq. (7) (Eurocode 2, 2004).

$$\begin{aligned} &\lambda = 0.8 && \text{for } f_{ck} \le 50\text{MPa} \\ &\lambda = 0.8 - (f_{ck} - 50)/400 && \text{for } 50 < f_{ck} \le 90\text{MPa} \end{aligned} \tag{6}$$

$$\begin{aligned} &\eta = 1.0 && \text{for } f_{ck} \le 50\text{MPa} \\ &\eta = 1.0 - (f_{ck} - 50)/200 && \text{for } 50 < f_{ck} \le 90\text{MPa} \end{aligned} \tag{7}$$

where, f_{ck} denotes the compressive strength of ULCC; ε_{cu} denotes the strain corresponding to ultimate compressive strength of the ULCC; f_y denotes the yield strength of the reinforcement.

4.2 Punching shear resistance of ULCC slab

Yan *et al*. (2016) developed some analytical models to calculate the punching shear resistance of ULCC flat slabs with reinforcements according modify the equations of predicting the punching shear resistance of slab in the code of ACI-318 (2014). The modified equation is as following:

$$P_{u,R} = \frac{1}{3}\frac{\left(0.28\rho_{SF} + 0.34\right)}{0.56} b_0 h_e \sqrt{f_{ck}} = \left(0.17\rho_{SF} + 0.20\right) b_0 h_e \sqrt{f_{ck}} \tag{8}$$

4.3 Ultimate resistance of the ULCC slab

According to the experiment results and the analytical results showed in Table 4, the ultimate resistance of the ULCC slab can be determined by the minor value of the punching shear resistance and flexure bending resistance as the following:

$$P_{u,T} = \min(P_{u,R}, P_{u,f}) \tag{9}$$

where, $P_{u,T}$ denotes the predicted ultimate resistance of the ULCC flat slabs; $P_{u,f}$ and $P_{u,R}$ are determined by Eq. (2) and Eq. (8), respectively.

4.4 Discussions

Table 4 compares the predictions of ultimate resistances by different approaches with the experimental values. For the slabs without flexural reinforcement that failed in flexure mode, i.e. S1~S3, it can be seen that the test-to-predictions by punching shear equations (Yan *et al*, 2016) are small and less than 0.33. This implies these slab failed in flexural bending mode prior to punching shear failure took place. Eq. (2) developed by yield line method offers an average test-to-prediction ratio of 1.06. This confirms the accuracy of the proposed model. For slabs S4~S8 that failed in punching shear mode, it can be seen that the predicted flexural bending resistance are much higher than the punching shear resistance. The average P_u-to-$P_{u,f}$ ratio is only 0.42. This agrees well with the experimental observations of punching shear failure occurred to S4~S8.

The modified ACI model (Yan *et al*, 2016) offers an average test-to-prediction ratio of 0.97 for slab S4~S8. Finally, the developed model [i.e. Eq. (9)] that considers both flexural bending resistance and punching shear resistance offers an average test-to-prediction ratio of 1.01.

5. Conclusions

This paper investigated the ultimate strength behaviours of the ULCC flat slabs adopting novel steel fibre reinforced ULCC with compressive strength around 85MPa and density around 1650kg/m^3. The four-specimen test program consists of three slabs with the flexural reinforcement and one slab without flexural reinforcement. All the specimens were loaded under concentrated patch loading. The influences of steel fibre content and loading area were studied in the test program. Theoretical analyses were carried out to predict the punching shear resistance and the flexure resistance of the ULCC slab based on the experiment results in this paper and some data that has been reported (Yan *et al*. 2016). These experimental investigations and analyses draw the following observations and conclusions:

1) The slabs without flexural reinforcement failed in flexure mode, and the load-deflection curves of the slabs without flexural reinforcement presented three distinct stages, i.e., elastic uncracked stage, nonlinear stage, and soften stage. And this failure mode is different from the punching shear failure mode of flat slabs with flexural reinforcement.

2) Flexural resistance and the elastic stiffness of the ULCC slabs increase with the increasing of the volume fraction of steel fibre. As the ρ_{SF} increased from 0.5% to 2%, the flexure resistance and the elastic stiffness increased by 76% and 17%, respectively.

3) The loading area could significantly influence the ultimate strength of ULCC flat slab. The $P_u/(h_e\sqrt{f_{ck}})$, ratio increased by 18% as the side width of loading area increased from 100 mm to 125 mm.

4) The yield line model was used to predict the flexural bending resistance of the ULCC slab. The equation for unit width bending moment resistance of ULCC without flexural reinforcement was modified in this paper. The comparison between the analysis results based on the modified equation and the test results showed the accurate of the modified equations and the yield line model. Finally, the design approach considering both punching shear resistance and flexural bending resistance was proposed to predict the ultimate resistance of the ULCC flat slabs with and without flexural reinforcement.

Acknowledgments

This work was supported by the National Nature Science Foundation of China [grant number 51609172, 51608358], the Fundamental Research Funds for the Central Universities, and Zhejiang Communication Science and Technology Project [grant number 2019-GXKY-01], and the Shanghai Municipal Science and Technology Project [grant number 17DZ1204200]. The financial supports are greatly appreciated.

References

Alexander, S.D.B. and Simmonds, S.H. (1987), “Ultimate strength of slab column connections”, *ACI Struct. J.*, **84**(3), 255-261.

American Concrete Institute 318-14 (ACI) (2014), Building Code Requirements for Structural Concrete (ACI 318-14) and Commentary, Farmington Hills (MI), American Concrete Institute; USA.

ASTM C39/C39M-14 (2014), Standard Test Method for Compressive Strength of Cylindrical Concrete Specimens, ASTM International; West Conshohocken, PA, USA.

ASTM A370-13 (2013), Standard Test Methods and Definitions for Mechanical Testing of Steel Products, ASTM International, West Conshohocken, PA, USA.

Chia, K.S., Zhang, M.H. and Liew, J.Y.R. (2011), “High-strength ultra-lightweight cement composite-material properties”, *9th International Symposium on High Performance Concrete-Design, Verification and Utilizaiton,* Rotorua, New Zealand, August.

Delahay, P.E.J. and Christopher, P.E.B. (2007), “Current trends in economical concrete construction, Part one: Floor framing and lateral systems”, *Struct. Mag.*, **7**, 19-21.

Eurocode 2 (2004), Design of concrete structures - Part 1-1: General Rules and Rules for Buildings, BS-EN-1992-1-1, European committee for Standardization; Brussels, Belgium.

Gardner, N.J., Huh, J. and Chung, L. (2002), “Lessons from the Sampoong department store collapse”, *Cement Concrete Compos.*, **24**(6), 23-29. https://doi.org/10.1016/S0958-9465(01)00068-3.

Kankam, C.K. and Odum, E.B. (2006), “Babadua reinforced concrete two-way slabs subjected to concentrated loading”, *Construction and Building Materials*, **20**(5), 279-285.

Liu, X.M., Chia, K.S., Zhang, M.H. and Liew, J.Y.R. (2012), “Water and chloride ion penetration resistance of high-strength ultra lightweight cement composite”, *1st International Congress on Durability of Concrete (ICDC)*, Trondheim, Norway, 18-21, June.

Rankin, G.I.B. and Long, A.E. (2015), “Predicting the punching strength of conventional slab-column specimens”, *Proceedings of the Institution of Civil Engineers Part Design & Construction*, **82**(2), 327-346.

Sohel, K.M.A., Liew, J.Y.R. and Zhang, M.H. (2011), “Analysis and design of steel-concrete composite sandwich systems subjected to extreme loads”, *Frontiers of Architecture and Civil Engineering in China September*, **5**(3), 278-293. https://doi.org/10.1007/s11709-011-0120-z.

Sohel, K.M.A., Liew, J.Y.R., Zhang, M.H., Yan, J.B. and Chia, K.S. (2013), “Investigation of longitudinal shear resistance of steel-ultra-lightweight cementitious composite slabs with profiled sheeting”, *10th International Conference on Advances in Steel Concrete Composite and Hybrid Structures*, Singapore, 2-4. July.

Schousboe, I. (1976), “Bailey’s crossroads collapse reviewed”, *J. Eng. Mech. Division*, **102**(2), 365-378.

Theodorakopoulos, D.D. and Swamy, R.N. (2002), “Ultimate punching shear strength analysis of slab column connections”, *Cement Concrete Compos.*, **24**(6), 509-521. https://doi.org/10.1016/S0958-9465(01)00067-1.

Wang, J.Y., Chia, K.S., Liew, J.Y.R. and Zhang, M.H. (2013), “Flexural performance of fibre reinforced ultra lightweight cement composites with low fibre content”, *Cement Concrete Compos.*, **43**, 39-47. https://doi.org/10.1016/j.cemconcomp.2013.06.006.

Wang, J.Y., Yang, Y., Liew, J.Y.R. and Zhang, M.H. (2014), "Method to determine mixture proportions of workable ultra lightweight cement composites to achieve target unit weights", *Cement Concrete Compos.*, **53**, 178-186. https://doi.org/10.1016/j.cemconcomp.2014.07.006.

Wang, J.Y., Gao, X.L. and Yan, J.B. (2018), "Developments and mechanical behaviors of steel fiber reinforced ultra-lightweight cement composite with different densities", *Construct. Build. Mater.*, **171**, 643-653. https://doi.org/10.1016/j.conbuildmat.2018.03.168.

Ward, P. (2010), "SFRC suspended slabs in flexure", *Struct. Eng.*, **88**, 16-19.

Yan, J.B., Liew, J.Y.R., Zhang, M.H. and Wang, J.Y. (2014), "Ultimate strength behaviour of steel-concrete-steel sandwich composite structures, Part 1: Experimental and analytical study", *Steel Compos. Struct.*, **17**(6), 907-927. https://doi.org/10.1617/s11527-014-0252-4.

Yan, J.B., Liew, J.Y.R., Zhang, M.H. and Sohel, K.M.A. (2015), "Experimental and analytical study on ultimate strength behaviour of steel-concrete-steel sandwich composite beam structures", *Mater. Struct.*, **48**, 1523-1544. https://doi.org/10.1617/s11527-014-0252-4.

Yan, J.B., Wang, J.Y., Liew, J.Y.R., Qian, X.D. and Zhang, W. (2016), "Reinforced ultra-lightweight cement composite flat slabs: Experiments and analysis", *Mater. Design*, **95**, 148-158. https://doi.org/10.1016/j.matdes.2016.01.097.

Yankelesky, D.A. and Leibowitz, O. (1999), "Punching shear in concrete slabs", *J. Mech. Sci.*, **41**(1), 1-15. https://doi.org/10.1016/S0020-7403(97)00086-6.

PL